We are IntechOpen,
the world's leading publisher of
Open Access books
Built by scientists, for scientists

4,800

Open access books available

122,000

International authors and editors

135M

Downloads

Our authors are among the

154

Countries delivered to

TOP 1%

most cited scientists

12.2%

Contributors from top 500 universities

CLARIVATE ANALYTICS
BOOK CITATION INDEX
INDEXED

WEB OF SCIENCE™

Selection of our books indexed in the Book Citation Index
in Web of Science™ Core Collection (BKCI)

Interested in publishing with us?
Contact book.department@intechopen.com

Numbers displayed above are based on latest data collected.
For more information visit www.intechopen.com

Accurate Receiver Model for Optical Fiber Systems with Polarization Induced Performance Degradation

Aurenice Oliveira
Michigan Technological University
USA

1. Introduction

Polarization-mode dispersion (PMD) and polarization-dependent loss (PDL) are the main polarization effects that degrade intermetropolitan and transoceanic high-speed optical fiber communication systems [Huttner et al., 2000]. As a result of the stochastic nature of PMD [Khosravani et al., 2001], it is very difficult to compensate the performance degradation due to PMD, which leads to waveform distortions and signal depolarization. Because PMD causes random fluctuations of the polarization state of the light, the performance degradation due to PDL also becomes stochastic; leading to power fluctuation in wavelength-division multiplexed (WDM) systems, and producing additional waveform distortions.

In this chapter, we demonstrate that one can use a semi-analytical receiver model to accurately estimate the performance of on-off-keyed (OOK) optical fiber communication systems, taking into account the impact of the choice of the modulation format, arbitrarily polarized noise, and the receiver characteristics [Lima Jr. et al., 2005]. We initially validate our semi-analytical model by comparing the results obtained with this model against experiments and extensive Monte Carlo simulations for cases in which the signal does not suffer significant waveform distortions, as in the case of negligible intra-channel PMD [Wang & Menyuk, 2001], [Lima Jr. et al. , 2003a]. For that case, we extend the work by [Marcuse, 1990], [Humblet & Azizoglu, 1991], and [Winzer et al., 2001] through the derivation of an expression that shows how the Q factor depends on both the electrical signal-to-noise ratio (SNR) and the optical signal-to-noise ratio (OSNR) for arbitrary modulation format and receiver characteristics. Marcuse's results [Marcuse, 1990], which have been widely used in the calculation of the Q-factor, only consider two extreme cases that the noise is unpolarized or copolarized with the signal. How the partially polarized noise, which happens in many optical systems with significant PDL [Wang & Menyuk, 2001], [Sun et al., 2003a], affects the system performance remains unclear. Therefore, in our next step we extend the Q-factor derived expression for the case in which the optical noise is partially depolarized due to PDL in long-haul optical fiber systems [Wang & Menyuk, 2001],[Lima Jr. et al., 2003a],[Sun et al., 2003a], [Sun et al., 2003b]. We systematically investigate effects of partially polarized noise in a receiver and compute the Q-factor using a general and accurate receiver model that takes into account the effect of partially polarized

noise as well as the optical pulse format immediately prior to the receiver and the shapes of the optical and electrical filters. Our results show that the system performance depends on both the degree of polarization of the noise (DOP) and the random angle between the polarization states of the signal and of the polarized part of the noise, i.e., the Stoke's vectors of the signal and the noise [Lima Jr. et al., 2005]. We also demonstrate that the relationship between the OSNR and the Q factor is not unique when the noise is partially polarized.

Finally, we show how to use our developed semi-analytical model to calculate the performance degradation in the presence of PMD-induced waveform distortions and the performance dependence on the receiver characteristics for different modulation formats [Lima Jr. & Oliveira, 2005]. In this study we focus on OOK optical fiber communication systems, which are the ones most widely used today because of their cost-effectiveness.

2. Modelling systems with negligible amount of intra-channel PMD

Undersea WDM systems that operate with speeds of up to 40 Gbit/s using ultra-low PMD fiber are not subject to waveform distortions due to PMD, but can suffer power fluctuations. In this case, PMD is not large enough to drift the spectral components within a single channel, but is sufficient to drift apart the polarization states of the WDM channels as the optical signal propagates down the transmission fiber [Wang & Menyuk, 2001]. The inter-channel polarization drift combines with PDL in the isolators and couplers of the erbium-doped optical amplifier subsystems, which leads to fluctuation in the power level of the channels. This power fluctuations cause performance degradations that can lead to outages [Lima Jr. et al., 2003a].

In the absence of waveform distortions due to PMD, and operation in the quasi-linear regime (that prevents inter-channel cross talk), the marks have a pulse shape that does not change overtime. We generalize a procedure introduced earlier by Winzer, *et al*. [Winzer et al., 2001] to show how one can derive an expression that determines the variance of the electric current due to arbitrarily polarized noise at the receiver. In this study, we neglect electrical noise at the receiver because optical transmission systems operate in the optimum regime with the use of optically preamplified receivers, which boost both the signal and the optical noise well above the electrical noise floor. The variance of the electric current $\sigma_i{}^2$ in the receiver has two components: one due to the noise-noise beating, and another due to the signal-noise beating. Therefore, the variance of the current at any time t has the form:

$$\sigma_i^2(t) = \left\langle i^2 \right\rangle(t) - \left\langle i \right\rangle^2(t) = \sigma_{ASE-ASE}^2(t) + \sigma_{S-ASE}^2(t) \tag{1}$$

The first component on the right isde of Eq. (1) is the variance of the electric current due to the noise-noise beating in the receiver, and is given by

$$\sigma_{ASE\text{-}ASE}^2 = \frac{1}{2} R^2 N_{ASE}^2 \frac{I_{ASE\text{-}ASE}}{\Gamma_{ASE\text{-}ASE}} \tag{2}$$

Where

$$\Gamma_{ASE\text{-}ASE} = \frac{1}{1 + DOP_n^2} \tag{3}$$

and

$$I_{\text{ASE-ASE}} = \int_{-\infty}^{+\infty} \left| r_o(\tau) \right|^2 r_e(\tau) \mathrm{d}\tau \tag{4}$$

and the expressions

$$r_o(\tau) = \int_{-\infty}^{+\infty} h_o(\tau') h_o^{\,*}(\tau + \tau') \mathrm{d}\tau' \tag{5}$$

and

$$r_e(\tau) = \int_{-\infty}^{+\infty} h_e(\tau') h_e(\tau + \tau') \mathrm{d}\tau' \tag{6}$$

are, respectively, the autocorrelation function of the optical and of the electrical filter at the receiver. In Eq. (3), DOP_n is the degree of polarization of the optical noise after the optical filter, and the noise-noise beating factor $\Gamma_{\text{ASE-ASE}}$ is the ratio between the variance of the current due to noise-noise beating (in the case that the noise is unpolarized) to the actual variance of the current due to noise-noise beating.

The second component of the variance of the electric current is due to the signal-noise beating, and is given by

$$\sigma_{\text{S-ASE}}^2(t) = R^2 N_{\text{ASE}} \Gamma_{\text{S-ASE}} I_{\text{S-ASE}}(t) \tag{7}$$

where

$$I_{\text{S-ASE}}(t) = 2 \int_{-\infty}^{+\infty} e_{s_o}(\tau) h_e(t - \tau)$$
$$\times \int_{-\infty}^{+\infty} e_{s_o}^*(\tau') h_e(t - \tau') r_o(\tau - \tau') \mathrm{d}\tau' \mathrm{d}\tau \tag{8}$$

The coefficient ,

$$\Gamma_{\text{S-ASE}} = \frac{1}{2} \left[1 + \text{DOP}_n \left(\mathbf{s}_s \cdot \mathbf{s}_n^{(p)} \right) \right] \tag{9}$$

is the signal-noise beating factor, which is the fraction of the noise that beats with the signal.

The performance of optical fiber systems is typically quantified by the bit-error-ratio (BER) or by the Q factor [Marcuse, 1990]. The Q factor, which is defined as a function of the mean and of the variance of the electric current at the receiver for the marks and for the spaces, is given by

$$Q = \frac{\langle i_1 \rangle - \langle i_0 \rangle}{\sigma_1 + \sigma_0} \tag{10}$$

Using the Gaussian approximation, which was validated in [Winzer et al., 2001], we can use the Q factor to calculate the BER by BER = $erfc(Q / \sqrt{2}) / 2 \cong \exp(-Q^2 / 2) / (\sqrt{2\pi}Q)$. The current mean is given by

$$\langle i \rangle(t) = i_s(t) + \langle i_n \rangle(t) \tag{11}$$

where $\langle \cdot \rangle(t)$ is the average over the statistical realizations of the noise at time t. Substituting Eq. (11) and Eq. (1) into Eq. (10), we now obtain Eq. (12), where t_1 and t_0 are the sampling times of the lowest mark and the highest space, respectively [Lima Jr. et al., 2005].

$$Q = \frac{[i_s(t_1) + \langle i_n \rangle] - [i_s(t_0) + \langle i_n \rangle]}{\left(\sigma_{S\text{-}ASE}^2(t_1) + \sigma_{ASE\text{-}ASE}^2\right)^{1/2} + \left(\sigma_{S\text{-}ASE}^2(t_0) + \sigma_{ASE\text{-}ASE}^2\right)^{1/2}} \tag{12}$$

Applying the expressions that we derived for the variance of the electric current at the receiver, which accounts for arbitrary modulation format, noise polarization state, extinction ratio α_e, and receiver characteristics, the Q factor can be expressed as

$$Q = \frac{(1 - \alpha_e)\xi \text{OSNR}(\Gamma_{ASE\text{-}ASE}\mu)^{1/2}}{\left(2\Gamma_{S\text{-}ASE}\Gamma_{ASE\text{-}ASE}\kappa_1\xi \text{OSNR} + 1\right)^{1/2} + \left(2\Gamma_{S\text{-}ASE}\Gamma_{ASE\text{-}ASE}\kappa_0\alpha_e\xi \text{OSNR} + 1\right)^{1/2}} \tag{13}$$

In Eq. (13),

$$\kappa_j = \frac{RB_o I_{S-ASE}(t_j)}{i_s(t_j) I_{ASE-ASE}} \tag{14}$$

κ_j (Eq. 14) is the signal-noise beating parameter for the marks ($j = 1$) and for the spaces ($j = 0$), and

$$\mu = \frac{2B_o^2}{I_{ASE\text{-}ASE}} \tag{15}$$

μ (Eq. 15) is the effective number of noise modes for the equivalent case in which the noise is unpolarized. The expression in Eq. (15) converges to the one in [Marcuse, 1990] for the simplified integrate and dump receiver with unpolarized noise that has been widely used in the literature.

The OSNR in Eq. (13) is defined by

$$\text{OSNR} = \frac{\langle |e_s(t)|^2 \rangle_t}{N_{ASE}B_{OSA}} \tag{16}$$

Where $\langle |e_s(t)|^2 \rangle_t$ is the time-averaged noiseless optical power per channel prior to the optical filter, and B_{OSA} is the noise equivalent bandwidth of an optical spectrum analyzer (OSA) that is used to measure the optical power of the noise. The parameter ξ in Eq. (13) and Eq. (17) is the enhancement factor [Lima Jr. et al., 2003b], which is used to express the Q-factor as a function of the OSNR, and is defined the as the ratio between the signal-to-noise ratio of the electric current of the marks SNR_1 and the OSNR at the receiver. The parameter ξ' in Eq. (17) is the normalized enhancement factor, which is equal to ξ when $B_{OSA} = B_o$.

$$\xi = \frac{\text{SNR}_1}{\text{OSNR}} = \frac{i_s(t_1)}{<i_n>} \frac{N_{ASE}B_{OSA}}{<|e_s(t)|^2>_t} = \xi' \frac{B_{OSA}}{B_o} \tag{17}$$

$$\xi' = i_s(t_1) / \left[R\langle |e_{in}(t)|^2 \rangle_t \right] \tag{18}$$

For a fixed SNR, the Q-factor is a function of the DOP of the noise and of the angle between polarization states of the signal and the polarized part of the noise. If the polarization state of the signal is fixed and the polarization states of the polarized part of the noise uniformly cover the Poincaré sphere, $\hat{\mathbf{s}} \cdot \hat{\mathbf{p}}$ is uniformly distributed between −1 and +1. In this situation, the probability density function (pdf) of the Q-factor is given by [Sun et al., 2003b]

$$f_Q(q) = \frac{1}{\kappa \mathrm{DOP}_n} \sqrt{\frac{\mu}{\Gamma_{ASE-ASE}}} \left(\frac{\mathrm{SNR}\sqrt{\Gamma_{ASE-ASE}\,\mu}}{q^3} - \frac{1}{q^2} \right), \quad q \in [Q_{min}, Q_{max}] \tag{19}$$

where Q_{max} and Q_{min} are given by substituting $\hat{\mathbf{s}} \cdot \hat{\mathbf{p}} = -1$ and $\hat{\mathbf{s}} \cdot \hat{\mathbf{p}} = +1$ in Eq. (9) and Eq. (13).

2.1 Modelling validation with simulations

In Figs. 1 and 2, we show the validation of Eq. (13) by comparison to Monte Carlo simulations with a large number of realizations in which the Q factor is computed using the standard time-domain formula $Q = (< i_1 > - < i_0 >) / (\sigma_1 + \sigma_0)$. For the results in Fig. 1, we used a back-to-back 10 Gbit/s optical system with unpolarized optical noise that was added prior to the receiver using a Gaussian noise source that has a constant spectral density within the spectrum of the optical filter. Since our study is focused on the combined effect that the pulse shape and the receiver have on the system performance, we did not include transmission effects here, such as those due to nonlinearity and dispersion.
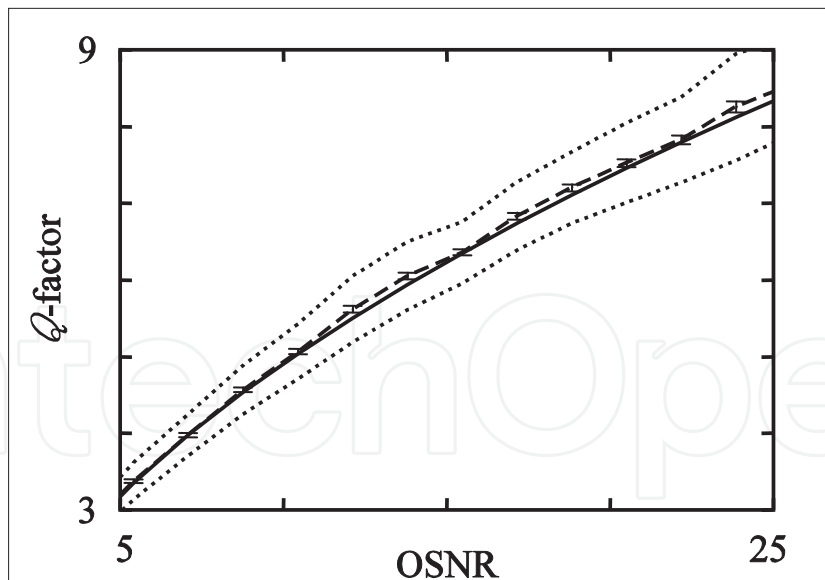

Fig. 1. Q factor as a function of the OSNR, in which the optical spectrum analyzer has a noise-equivalent bandwidth of 25 GHz. Validation of Eq. (13) (**solid line**) for the RZ raised-cosine format against Monte Carlo simulations with 100 Q samples each with 128 bits (**dashed line**). The **dotted line** shows the confidence interval in a single Monte Carlo simulation. The confidence interval is defined by the mean Q-factor plus and minus one standard deviation of the Q-factor, which gives an estimate of the error in the computation of the Q-factor using the time domain Monte Carlo method with a single string of bits.

In Fig. 1, we show the results using Eq. (13) with a solid line, which were obtained using only a single mark and a single space of the transmitted bit string. The results for the time-domain Monte Carlo method are shown with a dashed line. We obtained these results by averaging over 100 samples of the Q-factor, where for each sample the means and standard deviations of the marks and spaces were estimated using 128 bits. The agreement between the two methods is excellent.

For the results in Fig. 2, we used another back-to-back 10 Gbit/s system with partially polarized optical noise with $DOP_n = 0.5$ prior to the receiver. The partially polarized optical noise was obtained by transmitting unpolarized noise through a PDL element. We plot the Q-factor versus the OSNR for a linearly-polarized RZ raised-cosine signal with an optical extinction ratio of 18 dB. The curves show the results obtained using Eq. (13) and the symbols show the results obtained using Monte Carlo simulations. The solid curve and circles show the results when the polarized part of the noise is co-polarized with the signal.
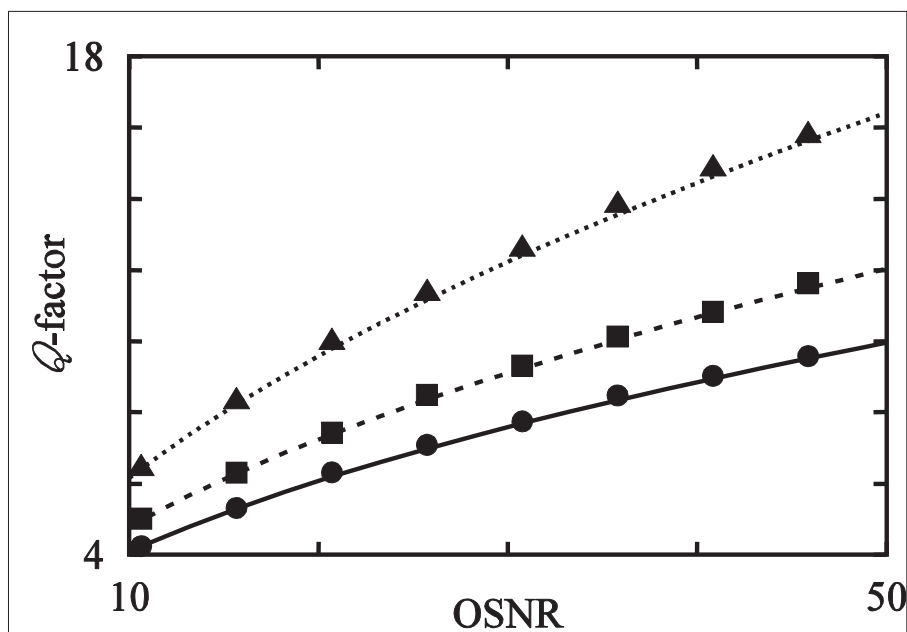

Fig. 2. Q factor as a function of the OSNR, in which the optical spectrum analyzer has a noise-equivalent bandwidth of 25 GHz. Validation of Eq. (13) (lines) with for the RZ raised-cosine format for different noise polarization states with $DOP_n = 0.5$. The solid line and the circles show results when the polarized part of the noise is co-polarized with the signal. The dashed lines and the squares and the dotted lines and triangels show results when the polarized part of the noise is in the left-circular and orthogonally polarized states to the signal, respectively.

The dashed curve and the squares, and the dotted curve and the triangles show the results when the polarized part of the noise is in the left circular and orthogonal linearly polarized states, respectively. Similarly to the results in Fig. 1, the agreement between Eq. (13) and Monte Carlo simulations in Fig. 2 is also excellent. When $DOP_n = 0.5$, the Q-factor varies by about 60% as we vary the polarization state of the noise. This variation occurs because the signal-noise beating factor $\Gamma_{S\text{-}ASE}$ in Eq. (9) depends on the angle between the Stokes vectors of the signal and the polarized part of the noise. The parameters in for this system are the

same ones in Fig.1 except that $\Gamma_{ASE-ASE} = 0.8$ and $\Gamma_{S-ASE} = 1$ for the solid line, $\Gamma_{S-ASE} = 0.5$ for the dashed line, and $\Gamma_{S-ASE} = 0.25$ for the dotted line. These results illustrate the significant impact that partially polarized noise can have on the performance of an optical fiber transmission system. Typical values for the PDL per optical amplifier in optical fiber systems range from 0.1 dB to 0.2 dB, which can partially polarize the optical noise in the transmission line.

2.2 Modelling validation with experimental results

In Fig. 3 we present a validation of Eq. (13) by comparison with back-to-back 10 Gbit/s experiments. The Q-factor versus the OSNR is obtained using both simulations and experiments for RZ and NRZ signals with unpolarized optical noise ($DOP_n < 0.05$) that is generated by an erbium-doped fiber amplifier without input power [Lima Jr. et al., 2005],[Sun et al., 2003b]. In Fig.3, the curves show results obtained using Eq. (13) and the symbols show the experimental results. The dot-dashed curve and the diamonds show the results for an RZ format with the electrical filter. The solid curve and circles show the results for the RZ format without the electrical filter. The dashed curve and squares show the results for the NRZ format with the electrical filter, and the dotted curve and triangles show the results for the NRZ format without the electrical filter. The parameters in Eq. (13) for the modulation formats shown in Fig.3 are described in Table 1.
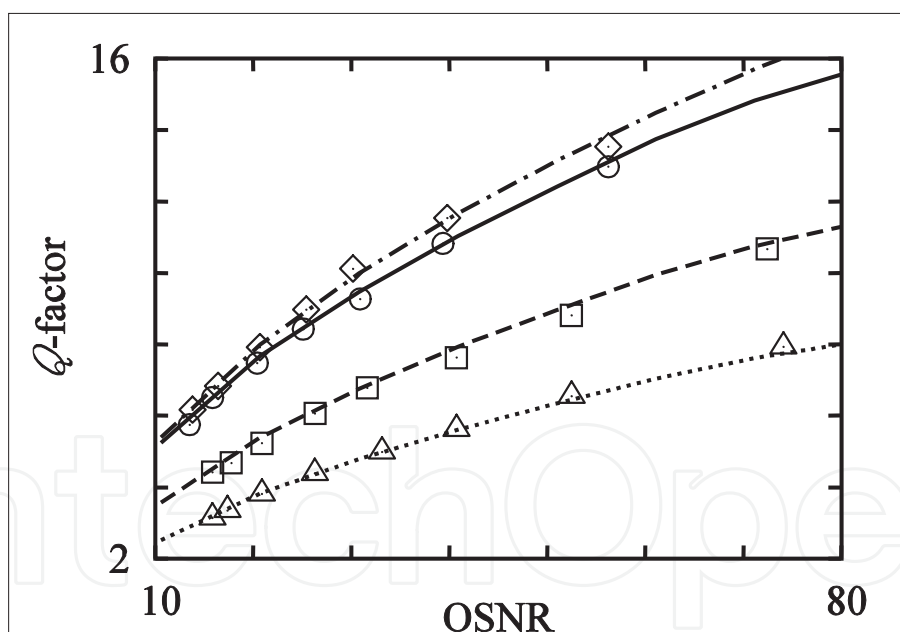

Fig. 3. Validation of Eq. (13) (lines) with experimental results (symbols). The dotted–dashed curve and the diamonds show the results for the RZ format with an electrical filter with a 3-dB bandwidth of 7 GHz. The solid curve and circles show the results for the RZ format without the electrical filter. The dashed curve and the squares show the results for the NRZ format with an electrical filter with a 3-dB bandwidth of 7 GHz. The dotted curve and the triangles show the results for the NRZ format without the electrical filter.

In Fig.3, we show that the performance of the RZ format is less sensitive than is the performance of the NRZ format to variations in the characteristics of the receiver. Since the

Format	α_e (dB)	ξ'	ξ	K_1	K_0	M
RZ with EF	−18.0	3.49	0.44	3.51	3.51	38.8
RZ w/o EF	−18.0	5.91	0.74	3.17	3.17	17.7
NRZ with EF	−11.3	1.89	0.24	2.88	2.68	38.8
NRZ w/o EF	−11.9	1.95	0.25	2.81	2.79	17.7

Table 1. Parameters of the modulation formats used in Fig. 3 with and without electrical filter (EF).

noise is unpolarized, $\Gamma_{ASE-ASE} = 1$, and $\Gamma_{S-ASE} = 0.5$. The results that we obtain using the formula Eq. (13) are in good agreement with the experimental results shown in this figure. An increase of the bandwidth of the electrical filter increases the amount of noise in the decision circuit which degrades the system performance. On the other hand, for systems with a 10 Gbit/s RZ format, increasing the electrical bandwidth from 7 to 15 GHz also reduces the broadening of the RZ pulses, and thereby increases the electric current due to the signal in the marks. However, this same effect does not occur in systems that use the NRZ format, since the NRZ pulses have a much narrower bandwidth.

In Fig. 4, we plot the Q-factor versus $\hat{\mathbf{s}} \cdot \hat{\mathbf{p}}$ when the noise is highly polarized and when it is partially polarized. The details of the experimental setup and schematic diagram are given in [Sun et al., 2003b].
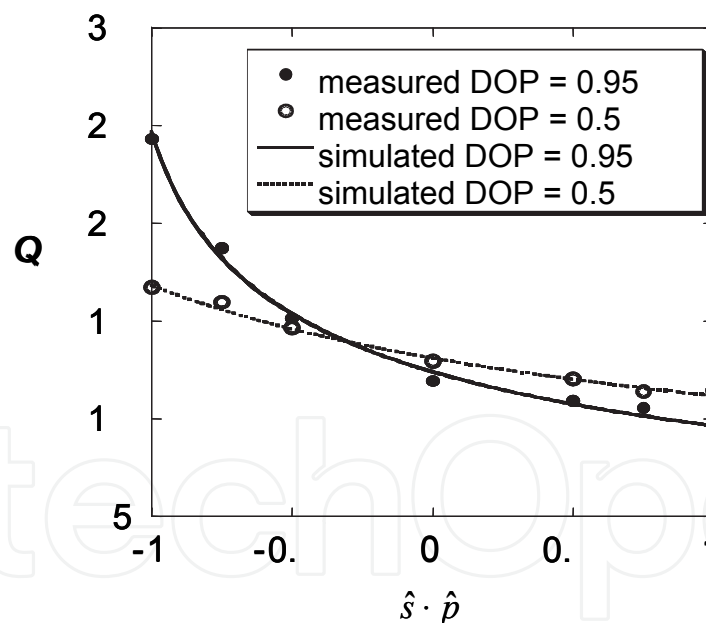

Fig. 4. The Q-factor plotted as a function of $\hat{\mathbf{s}} \cdot \hat{\mathbf{p}}$ [Sun et al., 2003b].

The experimental and analytical results we obtained when the DOP of the noise was set to 0.95 are shown with filled circles and a solid curve respectively. The corresponding results when the DOP of the noise is 0.5 are shown with open circles and a dotted curve. The agreement between theory and experiment is excellent. In both cases, the largest Q value occurs when the signal is antipodal on the Poincaré sphere to the polarized part of the noise and the signal-noise beating is weakest. Similarly, the smallest Q value occurs when the signal is co-polarized with the polarized part of the noise and the signal-noise beating is

strongest. Furthermore, as $\hat{\mathbf{s}} \cdot \hat{\mathbf{p}}$ is varied from −1 to +1 the variation in Q is less when the noise is partially polarized than when it is highly polarized.

In Fig.5, we measured the distribution of the Q-factor where the samples were collected using 200 random settings of the polarization controller (PC), chosen so that the polarization state of the polarized part of the noise uniformly covered the Poincaré sphere. The details of the experimental setup and schematic diagram are given in [Sun et al., 2003b]. We measured the Q-distribution when the DOP of the noise was DOP_n = 0.05, 0.25, 0.5, 0.75 and 0.95 when SNR = 12.3. In Fig. 5, we show the histogram of the measured Q-factor distribution with bars when DOP_n = 0.5, the corresponding result obtained using Eq. (19) with a solid curve, and the results obtained using a Monte Carlo simulation with 10,000 samples with a dotted curve. In the simulation, we chose the polarization states of the signal and of the polarized noise prior to the PC to be (1, 0, 0) in Stokes space and we used a random rotation after the polarized noise to simulate the PC. The 10,000 random rotations were chosen so that the polarization state of the polarized noise uniformly covered the Poincaré sphere. The theoretical and simulation results both agree very well with the experimental result. The sharp cut-offs in the Q-distribution at Q = 11.4 and Q = 17 correspond to the cases that the signal is respectively parallel and antipodal on the Poincaré sphere to the polarized part of the noise. The width $Q_{max} - Q_{min}$ of the Q-distribution depends on the DOP of the noise.
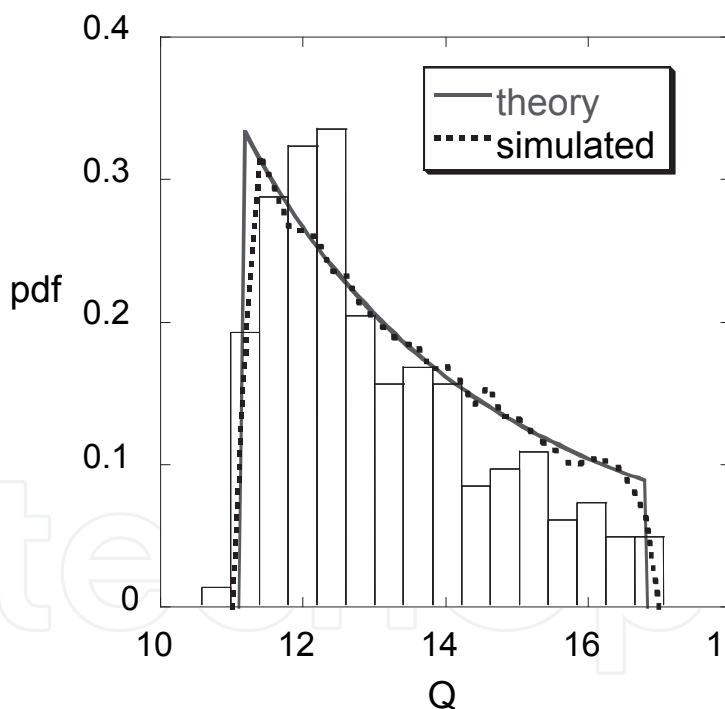

Fig. 5. The Q-factor distribution when DOP_n = 0.5 [Sun et al., 2003b].

In Fig. 6, we show the Q_{max}, Q_{min} and average Q factors as a function of the DOP of the noise, obtained both from measurements and analytically Eq. (19) [Sun et al., 2003b]. Although the average Q is not sensitive to a change in the DOP of the noise, the maximum and minimum Q values change dramatically with the DOP of the noise, especially the maximum Q values. The results shows that highly polarized noise will cause larger system variation than unpolarized noise.
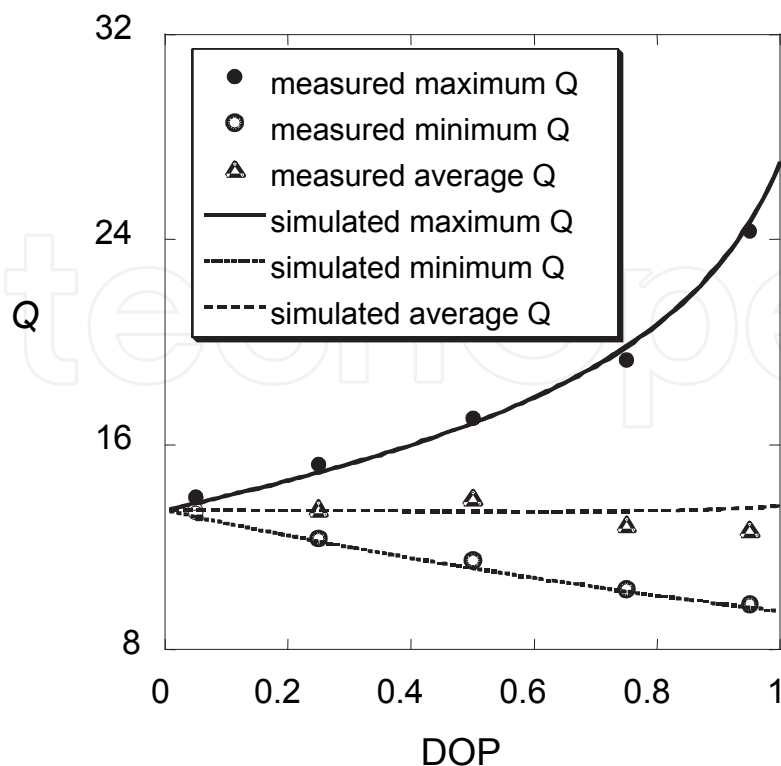
Fig. 6. The variation of the Q-factor as a function of the DOP of the noise. [Sun et al., 2003b].

The application of Eq. (13) for a particular system can enable the calculation of the power margin that can be allocated to different impairments and the calculation of the outage probability. This semi-analytical model can be combined with the reduced Stokes parameters model in [Wang & Menyuk, 2001], [Lima Jr. et al., 2003a] to determine the performance degradation that results from the combination of PDL and inter-channel PMD in transoceanic optical fiber transmission systems.

3. Modelling systems with significant intra-channel PMD

PMD is a polarization impairment that limits the data rate increase to 40 Gbit/s in a significant number of the optical fiber links built with high PMD coefficient fibers. PMD causes random waveform distortions that can produce outages in the communication channel. Because PMD distorts the waveform and leads to pattern dependences and even to inter-symbol interference, the BER cannot be calculated through the direct application of Eq.(10) and Eq.(13). Using the Gaussian approximation for each bit of a sufficiently long bit string enables the BER to be accurately calculated by [Lima Jr. & Oliveira, 2009]

$$
\begin{aligned}
\mathrm{BER}(t_s, i_{\mathrm{th}}) = & \\
& \frac{1}{N_0} \sum_{j=1}^{N_0+N_1} I_0(t_s+jT)\mathrm{erfc}\left[\frac{i_{\mathrm{th}}-i_s(t_s+jT)-\langle i_n\rangle}{\sqrt{2}\sigma_i(t_s+jT)}\right] \\
& + \frac{1}{N_0} \sum_{j=1}^{N_0+N_1} I_0(t_s+jT)\mathrm{erfc}\left[\frac{i_s(t_s+jT)+\langle i_n\rangle-i_{\mathrm{th}}}{\sqrt{2}\sigma_i(t_s+jT)}\right]
\end{aligned}
\tag{20}
$$

The instantaneous variance of the electric current in the receiver is given by,

$$\sigma_i^2(t) = \sigma_{\text{s-ASE}}^2 + \sigma_{\text{ASE-ASE}}^2 + \sigma_{\text{elec}}^2 \tag{21}$$

The first two terms in the right-hand-side of Eq. (21) are the signal-noise beating, and the noise-noise beating, respectively, the third term is due to the electrical noise in the receiver. Both the mean current due to noise in Eq. (20) and the noise-noise beating in Eq. (21) were computed as in Section 2. Because intra-channel PMD depolarizes the signal, the signal-noise beating must be computed using any two orthogonal decomposition of the Jones vector of the signal, which for unpolarized signal is given by [Lima Jr. & Oliveira, 2009]

$$\sigma_{\text{s-ASE}}^2(t) = R^2 N_{\text{ASE}} \times \left\{ \begin{array}{c} \iint e_x(\tau) h_e(t-\tau) e_x^*(\tau') h_e(t-\tau') r_o(t-\tau') d\tau' d\tau \\ + \iint e_y(\tau) h_e(t-\tau) e_y^*(\tau') h_e(t-\tau') r_o(t-\tau') d\tau' d\tau \end{array} \right\} \tag{22}$$

In Eq. (22), $e_x(t)$ and $e_y(t)$ are the horizontally and the vertically polarized components of the optically filtered noise-free signal, respectively, N_{ASE} is the noise spectral density prior to the optical filter, and R is the responsivity of the photodetector. The function $r_o(t)$ is the autocorrelation function of the impulse response of the optical filter and $h_e(t)$ is the impulse response of the electrical filter.

3.1 Simulation results

The power penalty was used as the performance measure. Once the BER in Eq. (20) is computed, the power penalty is calculated. The power penalty is defined as the input power increase in the system that produces the same performance observed in a PMD-free system that has optimized receiver filter bandwidths. The electrical filter bandwidth is defined as the 3-dB bandwidth and the optical filter bandwidth is specified as the full-width at half maximum (FWHM). The outage probability is the probability that the power penalty will exceed a specified penalty margin.

Using Eq. (21) into the value of σ_i^2 in Eq. (20), and considering unpolarized optical noise, we calculate the BER for 10 Gbit/s NRZ and raised-cosine RZ systems with optimized receiver filters. We consider -8 dBm of input optical signal, an optical noise spectral density of 0.60μW/GHz, and assuming a receiver with an equivalent electrical noise density of 31.5pW/Hz$^{1/2}$. The inclusion of the electrical noise is necessary in this study because its contribution increases with the electrical bandwidth. Since PMD is a linear effect, these results can be rescaled to 40 Gbit/s or to any other data rate. In Fig. 7, we show results of the power penalty with respect to the optimized receiver as a function of the receiver filter bandwidths. The optimized performances without PMD were obtained with optical filters with FWHM of 10 GHz for the NRZ format and 12 GHz for the RZ format, which are so narrow that they could result in additional penalty to the system due to detuning of the laser source wavelength, and the 3-dB electrical filter bandwidth was 12 GHz for both modulation formats. These results agree with earlier studies indicating the greater robustness of RZ systems when compared with NRZ systems with respect to the receiver characteristics [Winzer et al., 2001]. The performance advantage of RZ over the NRZ format is due to the larger enhancement factor that is characteristic of modulation formats with short duty cycle.
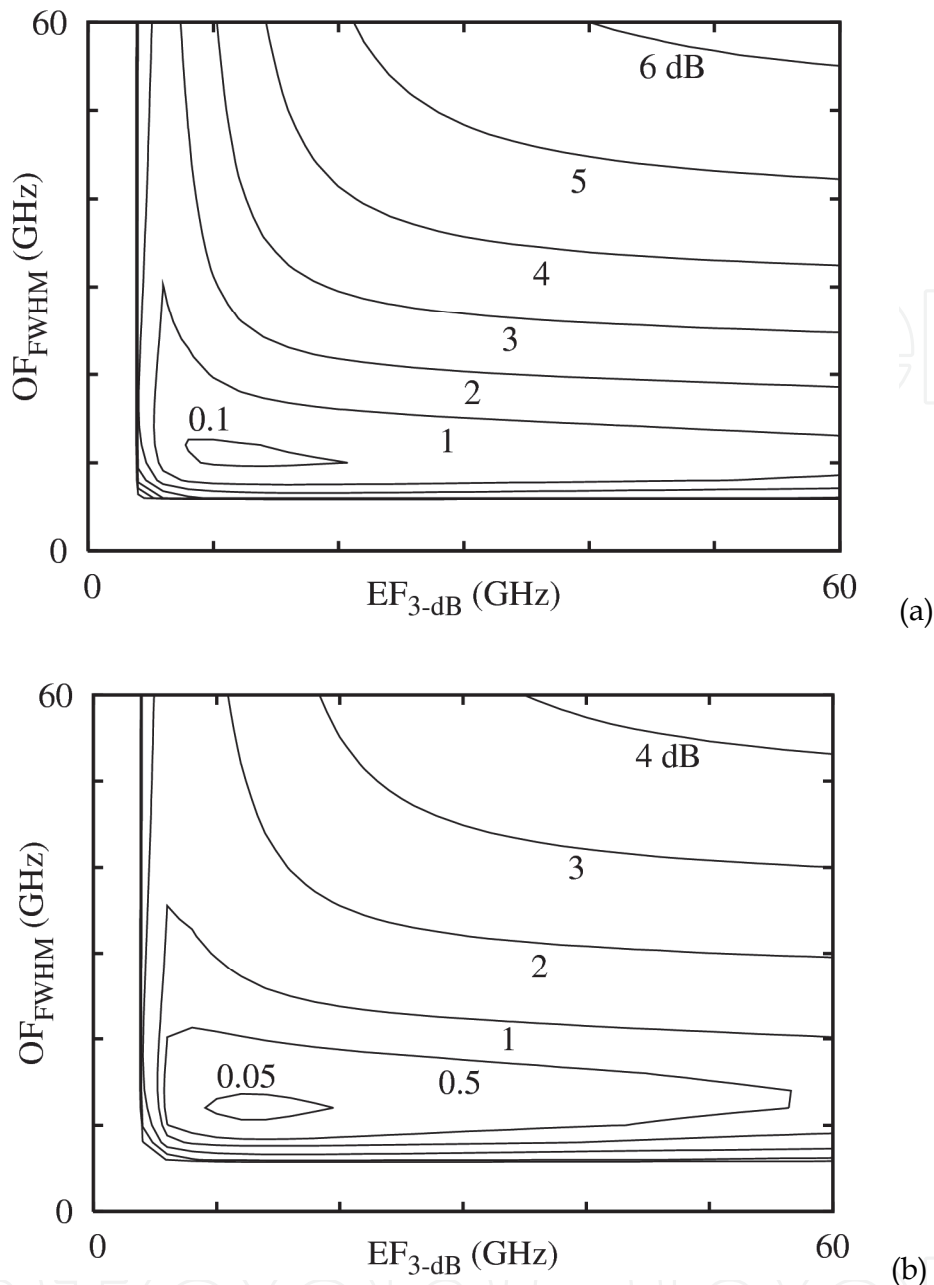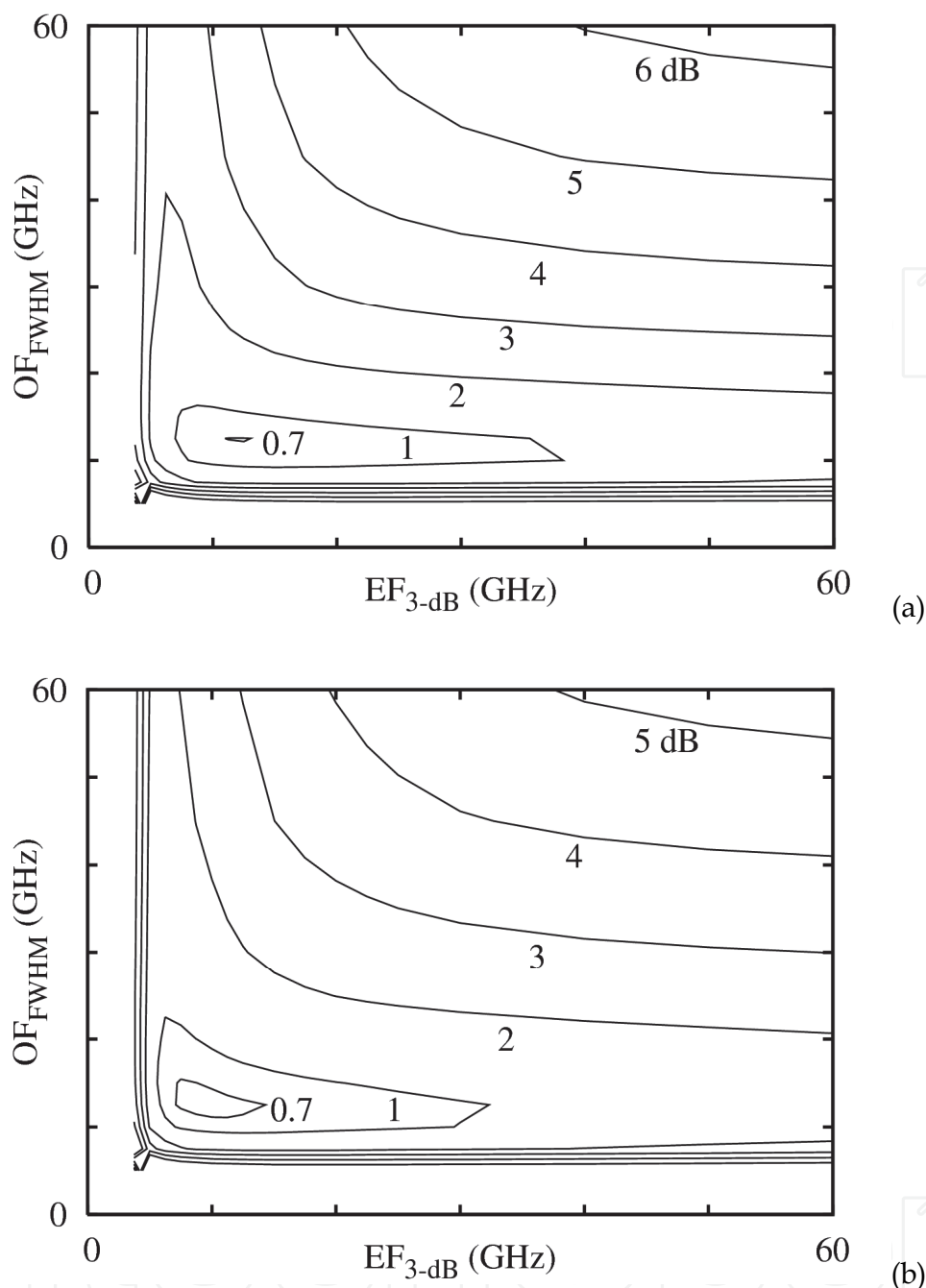
Fig. 7. Power penalty for (**a**) an NRZ system and (**b**) and RZ system with 10 Gbit/s without PMD as a function of the receiver filter bandwidths. The horizontal axis is the 3-dB bandwidth of the electrical filter and the vertical axis is the FWHM of the optical filter.

In Fig. 8, we use importance sampling in the Monte Carlo simulations of PMD [Biondini et al., 2002], [Oliveira et al., 2003] combined with the semi-analytical model in Eq. (13) to calculate the power penalty with respect to the optimized receiver at 10^{-5} outage probability level for the NRZ and raised-cosine RZ systems operating in a transmission fiber system with 10 ps of mean DGD (10% of the bit period). We observed that there is little difference between the optimum receiver filter bandwidths in the system with PMD and with PMD-free operation. In Fig. 8, we also observed a decrease of the robustness of the RZ system with respect to the receiver filter bandwidths. This effect results from the PMD-induced pulse broadening, which makes the RZ pulses to become similar to NRZ pulses.

Fig. 8. Power penalty for (**a**) an NRZ system and (**b**) and RZ system with 10 Gbit/s with a mean DGD of 10 ps as a function of the receiver filter bandwidths. The horizontal axis is the 3-dB bandwidth of the electrical filter and the vertical axis is the FWHM of the optical filter.

In Fig. 9, we show how an NRZ system with the receiver filters optimized for PMD-free operation and the receiver filters optimized for operation with mean DGD of 10 ps perform under different mean DGD values. Therefore, this system optimized for operation in the presence of PMD is operating in the sub-optimum regime in the cases in which the actual mean DGD is different from 10 ps. We observed only a small difference in the performance with the two optimized sets of filters, which reflects the small difference of the optimized receiver filter bandwidths for these two cases.
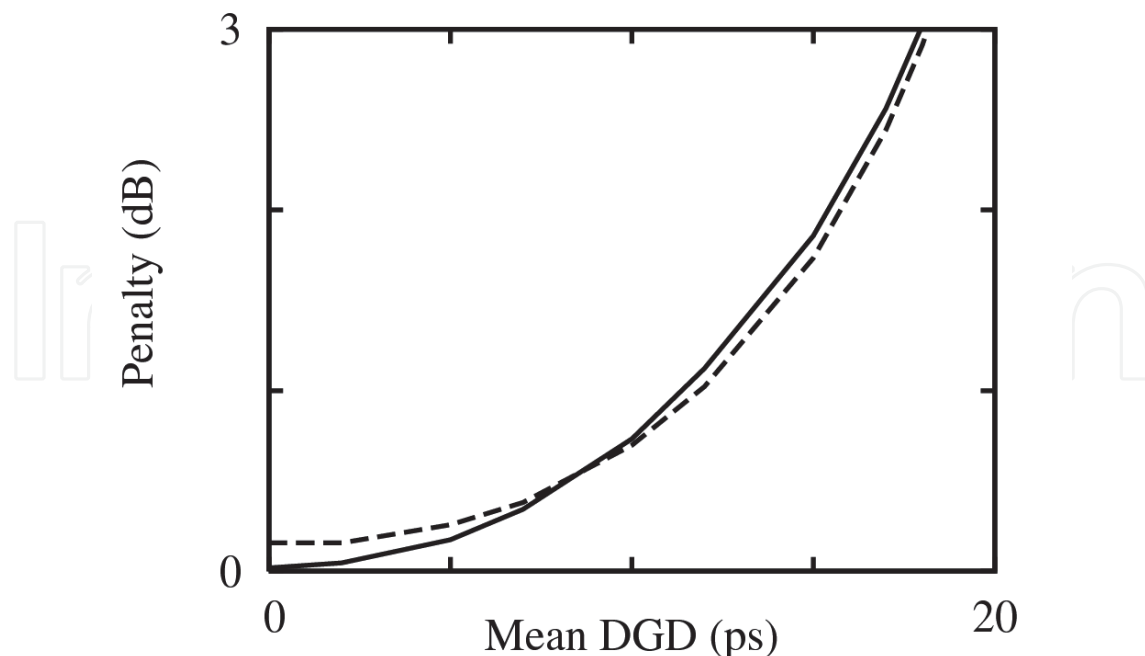
Fig. 9. Power penalty as a function of the mean DGD for an NRZ system. The solid line shows results for this system with optimized filter bandwidths in the absence of PMD. The dashed line shows results for the optimized filters for 10^{-5} outage probability in a system with mean DGD of 10 ps (10% of the bit period).

4. Conclusions

We used laboratory experiments and Monte Carlo simulations to show how one can use a semi-analytical receiver model to accurately calculate the Q factor for systems with arbitrary optical pulse shapes, arbitrary receiver characteristics, and arbitrary polarized noise. Our results showed that the system variation caused by partially polarized noise depends not only on the angle between the signal and polarized part of the noise but also on the DOP of the noise. Highly polarized noise will cause larger variation in the system performance. Our results suggest that in order to reduce the variation of the system performance, one needs to keep the noise unpolarized. The receiver model that we developed is also used to determine the performance degradation due to intra-channel PMD in optical fiber communication systems, and to show that the receiver filter bandwidths optimized for optical fiber systems at 10^{-5} outage probability due to PMD are very close to the ones optimized for the same systems in the absence of PMD. We observed that the PMD-induced waveform distortions significantly reduce the robustness of the RZ formats to the receiver characteristics. The receiver model that we developed can also be used to efficiently determine the performance degradation of optical fiber communication systems due to the combination of inter-channel PMD and PDL using the simplified reduced Stokes model.

5. Acknowledgment

The author thanks Dr. Yu Sun and Dr. Ivan Lima Jr. for helpful discussions, and for allowing the results of joint publications with the author (Dr. Aurenice Oliveira) to be used in this book chapter.

6. References

G. Biondini, W. L. Kath, and C. R. Menyuk, "Importance sampling for polarization-mode dispersion," *IEEE Photon. Technol. Lett.*, vol. 14, pp. 310-312, 2002.

B. Huttner, C. Geiser, and N. Gisin, "Polarization-induced distortions in optical fiber networks with polarization-mode dispersion and polarization-dependent losses," *IEEE J. Selec. Topics Quantum Electron.*, vol. 6, no. 2, pp. 317-329, Mar.-Apr. 2000.

P. A. Humblet and M. Azizoglu, "On the bit error rate of lightwave systems with optical amplifiers," *IEEE/OSA J. Lightwave Technol.*, vol. 9, no. 11, pp. 1576-1582, Nov. 1991.

R. Khosravani, I. T. Lima Jr. P. Ebrahimi, E. Ibragimov, A. E. Willner, and C. R. Menyuk, "Time and frequency domain characteristics of polarization-mode dispersion emulators," *IEEE Photon. Technol. Lett.*, vol 13, no. 2, Feb. 2001.

I. T. Lima Jr., A. M. Oliveira, Y. Sun, H. Jiao, J. Zweck, C. R. Menyuk, and G. M Carter, "A receiver model for optical fiber communication systems with arbitrarily polarized noise," IEEE/OSA J. Lightwave Technol., vol. 23., no. 3, pp. 1478-1490, Mar. 2005.

I. T. Lima Jr., A. M. Oliveira, J. Zweck, and C. R. Menyuk, "Efficient computation of outage probabilities due to polarization effects in a WDM system using a reduced Stokes model and importance sampling," *IEEE Photon. Technol. Lett.*, vol. 15, no. 1, pp. 45-47, Jan. 2003.

I. T. Lima Jr. and A. M. Oliveira, "Optimum receiver filters for optical fiber systems with polarization mode dispersion," IEEE/OSA J. Lightwave Technol., vol. 27, no. 14, pp. 2886-2891, Jul. 2009.

I. T. Lima Jr., A. M. Oliveira., J. Zweck, and C. R. Menyuk, "Performance characterization of chirped return-to-zero modulation format using an accurate receiver model," *IEEE Photon. Technol. Lett.*, vol. 15, no. 4, pp. 608-610, Apr. 2003.

D. Marcuse, "Derivation of analytical expression for the bit-error-probability in lightwave systems with optical amplifiers," *IEEE/OSA J. Lightwave Technol.*, vol. 8, no. 12, pp. 1816-1823, Dec. 1990.

A. M. Oliveira, I.T. Lima Jr., C. R. Menyuk, G. Biondini, B. S. Marks, and W. L. Kath, "Statistical analysis of the performance of PMD compensators using multiple importance sampling," *IEEE Photon. Technol. Lett.*, vol. 15, no. 12, pp. 1716-1718, Dec. 2003.

Y. Sun, A. M. Oliveira, I. T . Lima Jr., J. Zweck, L. Yan, C. R. Menyuk, and G. carter, "Statistics of the system performance in scrambled recirculating loop with PDL and PDG," *IEEE Photon. Technol. Lett.*, vol. 15, no. 8, pp. 1067-1069, Aug. 2003.

Y. Sun, I. T. Lima Jr., A. M. Oliveira, H. Jiao, J. Zweck, L. Yan, C. R. Menyuk, and G. Carter, "System performance variations due to partially polarized noise in a receiver," *IEEE Photon. Technol. Lett.*, vol. 15, no. 11, pp. 1648-1560, Nov. 2003.

D. Wang and C. R. Menyuk. "Calculation of penalties due to polarization effects in a long-haul WDM system using a stokes parameter model," *IEEE/OSA J. Lightwave Technol.*, vol 19, no. 4, pp. 487-494, Apr 2011.

P. Winzer, M. Pfnnigbauer, M. M. Strasser, and W. R. Leeb, "Optimum filter bandwidth for optically preamplified NRZ receivers," IEEE/OSA J. Lightwave Technol., vopl. 19, no. 9, pp. 1263-1273, Sep. 2001.
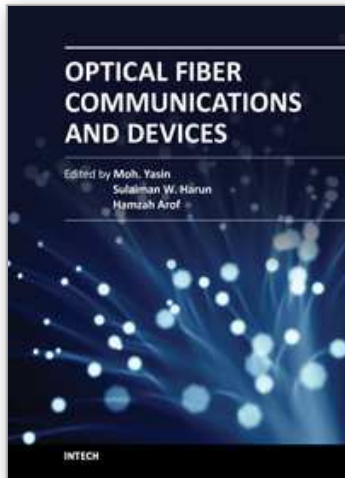
Optical Fiber Communications and Devices

Edited by Dr Moh. Yasin

This book is a collection of works dealing with the important technologies and mathematical concepts behind today's optical fiber communications and devices. It features 17 selected topics such as architecture and topologies of optical networks, secure optical communication, PONs, LANs, and WANs and thus provides an overall view of current research trends and technology on these topics. The book compiles worldwide contributions from many prominent universities and research centers, bringing together leading academics and scientists in the field of photonics and optical communications. This compendium is an invaluable reference edited by three scientists with a wide knowledge of the field and the community. Researchers and practitioners working in photonics and optical communications will find this book a valuable resource.

How to reference

In order to correctly reference this scholarly work, feel free to copy and paste the following:

INTECH

open science | open minds